

Organic light-emitting diodes with a spacer enhanced exciplex emission

Fei Yan, Rui Chen, Handong Sun, and Xiao Wei Sun

Citation: *Applied Physics Letters* **104**, 153302 (2014); doi: 10.1063/1.4871690

View online: <http://dx.doi.org/10.1063/1.4871690>

View Table of Contents: <http://scitation.aip.org/content/aip/journal/apl/104/15?ver=pdfcov>

Published by the [AIP Publishing](#)

Articles you may be interested in

[Efficient triplet harvesting by fluorescent molecules through exciplexes for high efficiency organic light-emitting diodes](#)

Appl. Phys. Lett. **102**, 153306 (2013); 10.1063/1.4802716

[Efficient organic light-emitting diodes through up-conversion from triplet to singlet excited states of exciplexes](#)

Appl. Phys. Lett. **101**, 023306 (2012); 10.1063/1.4737006

[Triplet annihilation exceeding spin statistical limit in highly efficient fluorescent organic light-emitting diodes](#)

J. Appl. Phys. **106**, 124510 (2009); 10.1063/1.3273407

[Highly efficient molecular organic light-emitting diodes based on exciplex emission](#)

Appl. Phys. Lett. **82**, 2209 (2003); 10.1063/1.1563838

[Oxadiazole-containing material with intense blue phosphorescence emission for organic light-emitting diodes](#)

Appl. Phys. Lett. **81**, 4 (2002); 10.1063/1.1491288

The advertisement features the 'physicstoday' logo in a bold, white font on a dark blue background. Below the logo, the text 'Comment on any Physics Today article.' is written in a large, white, serif font. A red arrow points from the text to a stack of three overlapping images of article pages. The top page is titled 'Measured energy in Japan' by David von Seggern. The middle page is titled 'The 1964 Chilean earthquake had 100 times more energy...' and discusses the energy release of the earthquake. The bottom page is titled 'Comment on 815.8936' and discusses the energy of a ball.

Organic light-emitting diodes with a spacer enhanced exciplex emission

Fei Yan,¹ Rui Chen,² Handong Sun,² and Xiao Wei Sun^{1,a)}

¹LUMINOUS! Center of Excellence for Semiconductor Lighting and Displays, School of Electrical and Electronic Engineering, Nanyang Technological University, 50 Nanyang Avenue, Singapore 639798

²Division of Physics and Applied Physics, School of Physical and Mathematical Sciences, Nanyang Technological University, Singapore 637371

(Received 29 March 2014; accepted 6 April 2014; published online 16 April 2014)

By introducing a spacer molecule into the blended exciplex emissive layer, the performance of the bulk heterojunction exciplex organic light-emitting diodes (OLEDs) was improved dramatically; the maximum luminous efficiency was enhanced by about 22% from 7.9 cd/A to 9.7 cd/A, and the luminous efficiency drop was reduced by 28% at 400 mA/cm². Besides the suppressed annihilation of exciton, the time-resolved photoluminescence measurements indicated that the spacer enhanced the delayed fluorescence through increasing the backward intersystem crossing rate from the triplet to singlet exciplex state. This method is useful for developing high performance exciplex OLEDs.

© 2014 AIP Publishing LLC. [<http://dx.doi.org/10.1063/1.4871690>]

Recently, organic light-emitting diode (OLED) display panels have become a viable display product in the market.^{1–5} On the other hand, OLED lighting development is relatively falling behind.^{6–8} For high quality OLED lighting, a high color rendering index is required. Generally, a broad band emission spectrum is preferred for high color rendering index.^{9,10} With a broad band emission originated from electronic transition between two different molecule species, exciplex based OLED should be a good candidate for high quality OLED lighting.^{11–15} However, compared to phosphorescent OLED, in general exciplex one has a lower luminous efficiency and faster efficiency roll-off.^{11–13} Improving the efficiency and its roll-off of exciplex OLED is important for exciplex based OLED lighting. In this work, we shall address these issues by introducing a spacer into the exciplex system. Significantly, improvement was obtained in terms of efficiency and its roll-off.

Exciplex can be defined as an exciton formed by Coulomb attraction between two oppositely charged molecules of different structures with type-II energy level alignment.^{16–18} These two molecule precursors forming the exciplex are called electron donor (D) and electron acceptor (A). The electron donor has a low ionization potential (the highest occupied molecular orbit (HOMO) of D is closer to the vacuum level than that of A), and the electron acceptor has a high electron affinity (the lowest unoccupied molecular orbit (LUMO) level is lower compared to D). Such two oppositely charged molecules are bonded by the Coulomb force and form the excited charge transfer complex (also called geminate pair¹⁸), a kind of weakly bonded charge transfer exciton (CTE).¹⁷ Such CTE could transform into exciplex exciton or free charge depending on temperature, electrical field, etc., and these three states can transit into each other.^{18,19} Additionally, the LUMO and HOMO of the charge transfer complex are primarily distributed on donor and acceptor, respectively, and separated by a relatively long distance, which leads to a very small energy difference

between S₁ and T₁ state.²⁰ Such characteristics facilitate the backward intersystem crossing from T₁ to S₁, i.e., rendering the long-lived delayed fluorescence.²⁰ Theoretically, the phenomena normally observed in regular OLEDs also exists in exciplex OLEDs, for example, the exciton annihilation caused by the exciton-exciton interaction.

Until now, a lot of works in enhancing exciplex-based OLEDs have been reported, including the utilization of exciplex emission directly and DA blended host for some high efficiency dopants.^{19,21,22} In this work, we selected 4,4',4''-tris(N-3-methylphenyl-N-phenyl-amino)triphenylamine (m-MTDATA) and 4,7-diphenyl-1,10-phenanthroline (Bphen) as the electron donor and acceptor, respectively. N,N'-di(naphthalene-1-yl)-N,N'-iphenyl-benzidine (NPB) was used as the spacer molecule. Other used chemical is cesium carbonate (Cs₂CO₃). Three OLEDs were fabricated on patterned tin-doped indium oxide (ITO) glass substrate (10 Ω/sq) in a single run without breaking the vacuum for comparison; Device A: ITO/m-MTDATA (50 nm)/Bphen (50 nm)/Bphen:Cs₂CO₃ (10% wt., 20 nm)/Al (100 nm), Device B: ITO/m-MTDATA (40 nm)/m-MTDATA:Bphen (1:1 wt., 20 nm)/Bphen (40 nm)/Bphen:Cs₂CO₃ (10% wt, 20 nm)/Al (100 nm), and Device C: ITO/m-MTDATA (40 nm)/m-MTDATA:Bphen:NPB (1:1: 8% wt., 20 nm)/Bphen (40 nm)/Bphen:Cs₂CO₃ (10% wt., 20 nm)/Al (100 nm). Device A is a control device with a planner heterojunction. Device B is another control device with a bulk heterojunction. Device C is the target device with an NPB doped bulk heterojunction emissive layer. The ITO substrates were cleaned with de-ionized water, isopropanol, acetone in sequence first. Then they were oven-dried and treated in O₂ plasma. All functional films and aluminum electrodes were fabricated by thermal evaporation in a single run at a base pressure of less than 4 × 10⁻⁴ Pa without breaking the vacuum. All the organics and Cs₂CO₃ were evaporated at a rate of about 0.1–0.2 nm s⁻¹, and the aluminum electrodes were evaporated at a rate of 0.8–1 nm s⁻¹. A shadow mask was used to define the cathode and we could obtain eight devices (with emissive area of 4 × 4 mm²) on each substrate. The luminance-current-voltage (L-I-V) characteristics and electroluminescence (EL) spectra were

^{a)}Author to whom correspondence should be addressed. Electronic mail: exwsun@ntu.edu.sg.

measured simultaneously with a Keithley 2400 source meter and a Photoresearch PR-650 spectrometer. The photoluminescence (PL) experiment was performed on the m-MTDATA:Bphen:NPB (1:1:x% wt., 30 nm) films deposited on quartz substrate. A third harmonic Nd:YAG laser (355 nm) with a pulse width and repetition rate of 5 ns and 20 Hz was used as the excitation source, and the signal was dispersed by a 750 mm monochromator combined with suitable filters, and detected by a photomultiplier tube (Hamamatsu R928) using standard lock-in amplifier technique. For the luminescence decay experiment, the detector output was stored by a digital phosphor oscilloscope (Tektronix DPO 7254) and averaged over 500 periods to improve the signal-to-noise ratio. All measurements were carried out at room temperature in ambient atmosphere.

Figure 2 shows the normalized PL spectra of m-MTDATA, Bphen, and exciplex, as well the normalized EL spectra of devices A, B, and C. It can be seen from Fig. 1 that the emission from the two precursors cannot be observed and a new broad band emission peaking at about 560 nm appears originating from the exciplex formed by the donor (m-MTDATA) and the acceptor (Bphen), consistent with the literatures.^{16–19,21,22} As shown in Fig. 1, the EL spectra of the three devices are almost the same, and their shape are very similar with the PL spectrum. Additionally, the emission from the two precursors cannot be observed in EL spectra, thus all emissions are originated from the exciplex.^{16–19,21,22} Furthermore, it is noted that the spectrum line width of EL is slightly broader and redshifted compared to the PL spectrum. As EL is obtained under external electrical bias, the broadening and redshifting of the EL spectrum are probably related to the Stark Effect caused by the external field.^{23,24}

As shown in Fig. 2, the turn on voltage of all exciplex OLEDs is low, which is about 2.2 V (the energy of 560 nm photon is about 2.2 eV), indicating that the charges can inject and transport to the recombination zone almost without any energy barrier. In fact, with its HOMO close to the work function of ITO, m-MTDATA plays a good role of anode buffer layer to lower down the hole injection barrier

effectively. The utilization of n-type doped electron injection layer of Bphen:Cs₂CO₃ decreases the barrier of electron injection from Al cathode. The lower driving voltage is an advantage of exciplex OLEDs comparing to the conventional OLEDs. In the blended structure of Device B, the charge transport path was influenced negatively by the introduction of another precursor because both the charge carrier transport paths were blocked partially, which leads to a higher driving voltage (2.91 V at 1 mA/cm²) comparing to the planar structure Device A (2.84 V at 1 mA/cm²). Similarly, for Device C, the addition of spacer NPB caused a further increase of driving voltage (3.25 V at 1 mA/cm²), especially for the electrons because of the low electron mobility and the high-lying LUMO of NPB.

In Device A with a planar DA heterojunction, because the high energy barrier for electron and hole at the DA heterojunction interface, almost all charge carriers injected are concentrated at the two sides of the interface. Therefore, the recombination zone was localized within a very narrow region at the interface about two molecules in thickness, leading to a small amount of CTE recombination but a large number of polarons. As the driving current increases, the densities of charge carriers increase correspondingly at the interface. Such high density of charge carriers caused an intense polaron-exciton interaction, leading to serious quenching of the CTE and exciplex exciton, and hence a fast efficiency drop-off as shows in Fig. 2.²⁵ In Device B with a bulk heterojunction, the DA heterojunction interface distributes in the blended layer uniformly, thus the amount of emission center increases significantly comparing to Device A. As shown in Fig. 2, the luminous efficiency of Device B is comparable to that of Device A at low current density, but significantly higher at high current density; the luminous efficiency shows a smaller roll-off for Device B. In Device B, the CTE and exciplex exciton exist in the whole bulk heterojunction emissive layer, which resembles the situation of a low efficiency OLED with un-doped emissive layer.²⁶ The dipole-dipole interaction is strong as the dipole moment of the CTE is larger than that of a localized molecular exciton, leading to serious exciton-exciton annihilation, especially

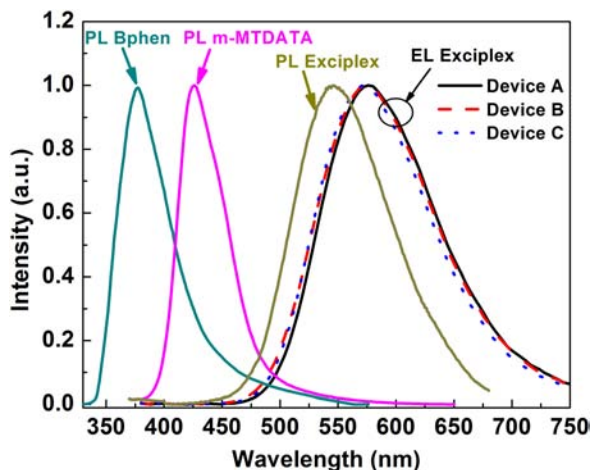


FIG. 1. The normalized photoluminescence spectra of m-MTDATA, Bphen, and exciplex; and the normalized electroluminescence spectra of devices A, B, and C at a driving current density of 1 mA/cm².

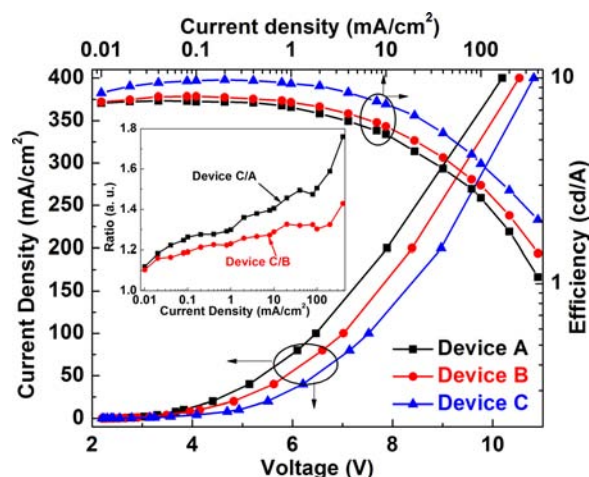


FIG. 2. The current density-voltage and luminous efficiency-current density curves of devices A, B, and C. The luminous efficiency ratios plots of Device C to Device B (red circle) and Device C to Device A (black square) are shown in inset.

under high driving current density, thus the efficiency roll-off is fast. Furthermore, the binding of such CTE is much weaker than that of localized molecular exciton, therefore, the influence of external field should be more significant, leading to a more serious dissociation of the CTE with the presence of the external bias.^{17,18,23,24,27} As reported, to suppress the exciton-exciton annihilation, almost all high efficiency OLEDs are using a doped emissive layer structure which keeps a suitable distance between neighboring excitons, especially for the phosphorescent devices with longer triplet exciton lifetime.¹⁹ To reduce the exciton-exciton annihilation, we introduced a spacer (S) molecule into the blended m-MTDATA:Bphen emissive layer (Device C). In order to avoid generating any new kind of CTE, we selected a classical blue emission (440 nm) hole transport material NPB as the spacer, considering its energy levels with respect to that of Bphen. On the other hand, as the exciplex is an intermolecular charge transfer process, on which the spacer will have adverse effect. Thus, there should be an optimal ratio of NPB to donor (or acceptor). In our experiment, we used a D:A:S weight ratio of 1:1:8%. As indicated in Fig. 2, though the added NPB molecules influence the formation of CTE, leading to a decrease in the density of emission centers slightly, the exciton-exciton annihilation was also suppressed effectively through separating neighboring excitons by a longer distance. Overall, the maximum luminous efficiency was still enhanced by about 26% and 22% to about 9.7 cd/A comparing to the Device A and B, respectively. Additionally, as the inset of Fig. 2 indicates, both the luminous efficiency ratios of Device C to Device A and Device C to Device B increase with the increase of the driving current density, indicating that the efficiency drop of Device C is lower comparing to Device A and Device B; the efficiency drop of Device C is reduced by 54% and 28% comparing to Device A and Device B at 400 mA/cm², respectively.

To furthermore study the enhancement of the device by NPB spacer, a systematic spectroscopy investigation of transient PL experiments was performed. In order to avoid the emission from precursors and spacer molecules, the detected wavelength was selected at 600 nm in the transient PL testing. Fig. 3 shows the luminescence decay plots of the m-MTDATA:Bphen:NPB (1:1: x% wt, x = 0, 5, 10, and 20) film at room temperature. The decay curves can be well-fitted by an exponential fit with reconvolution

$$I(t) = \int_{-\infty}^t IRF(t') A e^{-(t-t')/\tau} dt', \quad (1)$$

where A is the amplitude of the component at time zero, τ is the corresponding lifetime, and IRF is the instrument response function. It can be seen from Fig. 3 that, in all films the exciplex emission contains two components with different excited state lifetimes, though their emissive spectra are identical. For all films, the excited state lifetimes of the prompt component almost keep a constant value of 32 ns, which is due to the singlet exciplex exciton relaxation. The slower one with a lifetime comparable to classical phosphorescence emission originates from the long-lived delayed fluorescence.^{20,28,29} As indicated in Fig. 3 (inset (a)), it is interesting that the decay rate of the delayed component

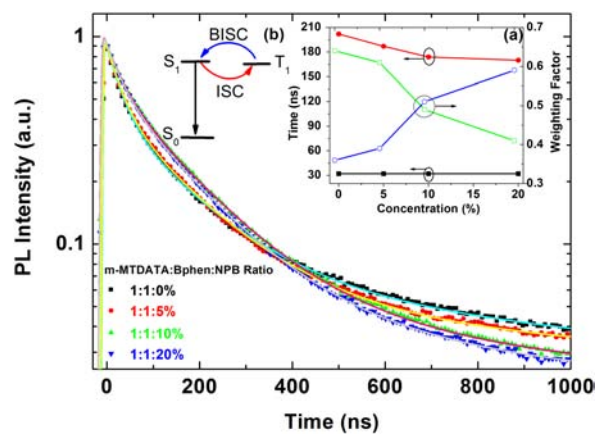


FIG. 3. The transient photoluminescence plots (focus on 600 nm) of the m-MTDATA:Bphen:NPB (1:1: x% wt., 30 nm) film ($x = 0, 5, 10,$ and 20), and the solid lines are correspondingly fitting curves. Through two exponential fitting, two components were observed in all films emission. The inset (a) indicates the plots of the lifetime of the prompt component (black solid square) and the delayed one (red solid circle) versus NPB concentration and their weighting factor variations of prompt component (green empty square) and delayed one (blue empty circle) as NPB concentration increases. The inset (b) shows the intercrossing crossing (ISC) from singlet (S_1) to triplet exciplex state (T_1) and the backward ISC (BISC). S_0 is the ground state.

becomes faster (from 202 ns to 170 ns) after adding the spacer molecule NPB into the blended film, and the weighting factor (the ratio of amplitude of the two components) of the delayed component increases with the increase of the NPB composition. Considering there is no energy acceptor or other quencher in this blended film, we concluded that the addition of spacer molecule NPB into the blended films probably enhanced the backward intercrossing crossing (ISC) rate from the triplet (T_1) to singlet exciplex state (S_1) (Fig. 3 inset (b)). Obviously the shorter T_1 lifetime lowers down the annihilation of triplet exciplex exciton, which is beneficial to suppressing efficiency roll-off at high driving current density. Additionally, the enhanced backward ISC rate from T_1 to S_1 also plays an important role in device performance improvement.

In conclusion, we have investigated the exciplex emission of OLEDs with a spacer. Due to the high density of charge carrier and exciton-exciton interaction, both the planar heterojunction and bulk heterojunction devices showed lower luminous efficiency. By introducing a spacer molecule into the blended emission layer of the bulk heterojunction device, both the maximum luminous efficiency and roll-off at high driving current density were improved significantly. Through the systematic spectroscopy investigation, it is implied that the spacer not only suppressed the exciton annihilation but also enhanced the delayed fluorescence of exciplex. Our work shed light on the high performance exciplex OLEDs.

This work was financially supported by National Research Foundation (Grant Nos. NRF-CRP11-2012-01 and NRF-CRP6-2010-2).

¹S. Kalluri, R. R. Jerry, and C. Charles, *Conference on Head- and Helmet-Mounted Displays XVII/Conference on Display Technologies and Applications for Defense, Security, and Avionics VI*, Baltimore, MD, 25–26 April 2012.

- ²Z. Ma, P. Sonar, and Z. Chen, *Curr. Org. Chem.* **14**, 2034–2069 (2010).
- ³A. Laaperi, *J. Soc. Inf. Disp.* **16**, 1125–1130 (2008).
- ⁴O. N. Ermakov, M. G. Kaplunov, O. N. Efimov, and S. A. Stakharny, *Proc. SPIE* **6636**, A6360 (2007).
- ⁵A. Laaperi, I. Hyytiäinen, T. Mustonen, and S. Kallio, *Dig. Tech. Pap. - Soc. Inf. Disp. Int. Symp.* **38**, 1183–1187 (2007).
- ⁶Y. Chang and Z. Lu, *J. Disp. Technol.* **9**, 459–468 (2013).
- ⁷M. Mazzeo, F. Mariano, A. Genco, S. Carallo, and G. Gigli, *Org. Electron.* **14**, 2840–2846 (2013).
- ⁸Y. H. Son, M. J. Park, Y. J. Kim, J. H. Yang, J. S. Park, and J. H. Kwon, *Org. Electron.* **14**, 1183–1188 (2013).
- ⁹T. W. Koh, H. Cho, C. Yun, and S. Yoo, *Org. Electron.* **13**, 3145–3153 (2012).
- ¹⁰J. N. Yu, H. Lin, F. F. Wang, Y. Lin, J. H. Zhang, H. Zhang, Z. X. Wang, and B. Wei, *J. Mater. Chem.* **22**, 22097–22101 (2012).
- ¹¹Y. Zhao, L. Duan, X. Zhang, D. Q. Zhang, J. Qiao, G. F. Dong, L. D. Wang, and Y. Qiu, *RSC Adv.* **3**, 21453–21460 (2013).
- ¹²H. J. Ji and J. G. Jang, *15th International Symposium on Advanced Display Materials and Devices (ADMD), Kumamoto University, Kumamoto, Japan, June 30–July 1* (2011).
- ¹³K. S. Lee, D. C. Choo, and T. W. Kim, *Thin Solid Films* **519**, 5257–5259, (2011).
- ¹⁴L. C. Palilis, A. J. Mäkinen, M. Uchida, and Z. H. Kafafi, *Appl. Phys. Lett.* **82**, 2209 (2003).
- ¹⁵S. L. Lai, M. Y. Chan, Q. X. Tong, M. K. Fung, P. F. Wang, C. S. Lee, and S. T. Lee, *Appl. Phys. Lett.* **93**, 143301 (2008).
- ¹⁶T. Granlund, L. A. A. Pettersson, M. R. Anderson, and Olle Inganäs, *J. Appl. Phys.* **81**, 8097 (1997).
- ¹⁷X. Y. Zhu, Q. Yang, and M. Muntwiler, *Acc. Chem. Res.* **42**, 1779–1787 (2009).
- ¹⁸A. C. Morteani, P. Sreearunothai, L. M. Herz, R. H. Friend, and C. Silva, *Phys. Rev. Lett.* **92**, 247402 (2004).
- ¹⁹Y. Park, S. Lee, K. Kim, S. Kim, J. Lee, and J. Kim, *Adv. Funct. Mater.* **23**, 4914–4920 (2013).
- ²⁰K. Goushi and C. Adachi, *Appl. Phys. Lett.* **101**, 023306 (2012).
- ²¹D. Wang, W. Li, B. Chu, Z. Su, D. Bi, D. Zhang, J. Zhu, F. Yan, Y. Chen, and T. Tsuboi, *Appl. Phys. Lett.* **92**, 053304 (2008).
- ²²H. Chen, C. Liao, H. Su, Y. Yeha, and K. Wong, *J. Mater. Chem. C* **1**, 4647–4654 (2013).
- ²³M. Yokoyama, Y. Endo, and H. Mikawa, *Chem. Phys. Lett.* **34**, 597–600 (1975).
- ²⁴Y. Takehara, N. Ohta, S. Shiraishi, S. Asaoka, T. Wada, and Y. Inoue, *J. Photochem. Photobiol. A: Chem.* **145**, 53–60 (2001).
- ²⁵S. Reineke, K. Walzer, and K. Leo, *Phys. Rev. B* **75**, 125328 (2007).
- ²⁶M. Sun, J. Jou, W. Weng, and Y. Huang, *Thin Solid Films* **491**, 260–263 (2005).
- ²⁷F. Yan, H. Liu, W. Li, B. Chu, Z. Su, G. Zhang, Y. Chen, J. Zhu, D. Yang, and J. Wang, *Appl. Phys. Lett.* **95**, 253308 (2009).
- ²⁸H. Uoyama, K. Goushi, K. Shizu, H. Nomura, and C. Adachi, *Nature* **492**, 234–238 (2012).
- ²⁹J. J. Benson-Smith, J. Wilson, C. Dyer-Smith, K. Mouri, S. Yamaguchi, H. Murata, and J. Nelson, *J. Phys. Chem. B* **113**, 7794–7799 (2009).